1 **Interaction between East Asian summer monsoon and west winds as**

2 **shown by tree-ring records**

4 Shengchun Xiao[1*], Xiaomei Peng[1], Quanyan Tian[1], Aijun Ding[2], Jiali Xie[1], Jingrong

5 Su[1][3]

7 [1] Key Laboratory of Ecological Safety and Sustainable Development in Arid Lands,

8 Northwest Institute of Eco-Environment and Resources, Chinese Academy of

9 Sciences, Lanzhou, Gansu, China 730000.

10 [2] College of Resources and Environment, Gansu Agricultural University, Lanzhou,

11 Gansu, China 730070.

12 [3] University of Chinese Academy of Sciences, Beijing, China 100049.

13 * Corresponding author (xiaosc@lzb.ac.cn).

14 Address: 320 West Donggang Road, Lanzhou City, Gansu Province, China.

15 Zip Code: 730000.

Abstract:

Against the background of changes in global atmospheric circulation, local changes in the East Asian summer monsoon (EASM) and the mid-latitude westerly winds will inevitably affect the climate and ecology of the arid zone of Northwest China. Hence, it is important to study these changes. We chose to observe these changes in the Alxa Plateau using dendrochronological methods. We assembled ring-width records from Qinghai spruce trees growing in the mountain regions surrounding the Alxa Plateau: the Helan Mountains, Changling Mountain, and Dongdashan Mountain. We analyzed these records for changes on interannual and interdecadal scales. Our results show that radial growth was indeed affected by changes in the monsoons and westerlies. The heterogeneity of precipitation and climatic wet-dry changes in different regions is primarily influenced by the interactions between atmospheric circulation systems, each with its own dominant controlling factors. In the case of the Helan Mountains, both of these major atmospheric circulation systems play a significant role in shaping climate changes. Changling Mountain in the southern part of the Alxa Plateau are mainly influenced by the EASM. Dongdashan Mountain is mainly influenced by the westerlies. Understanding these local conditions will help us predict climate changes in Northwest China.

Key words: Alxa Plateau, dendroclimatology, westerly winds, EASM, interaction between winds and monsoon

1. Introduction

1.1 Importance of climate studies in northwestern China

The alpine zone of Qinghai-Tibet, the arid zone of the northwestern interior, and the humid zone of the east constitute the three main areas of China's natural geomorphology (Chen et al., 2019b). The Northwest China inland dry zone is located in the hinterland of the Eurasian continent and is among the driest regions in the world. It exhibits typical continental climatic characteristics. This region is mainly influenced by westerly winds and the EASM. The interaction of these two factors results in high precipitation variability and hence frequent droughts. This would be the case even before global climate change began affecting the area; it is even more the case in current years. This inland dry zone is very much an ecologically fragile area (Chen et al., 2019a; Chen et al., 2019b; Zhang et al., 2023).

The semi-arid and arid regions of northern China are characterized by large areas of sand and desert. They are the second largest source of dust in the world after the Sahara. Their contribution to global climate change is large. So far inland, the influence of the EASM is often weak (Zhang et al., 2021; Liu et al., 2022). It is opposed by the westerly winds that flow from the North Atlantic climate zone toward the East Asian monsoon climate zone (Qu et al., 2004). The interaction between the westerly winds and the EASM governs precipitation, water vapor transport, and thus the climate of northwestern China (Feng et al., 2004; Wang et al., 2005; Li et al., 2008; Ma et al., 2011).

It is important to understand the history of this interaction if we are to estimate how global climate change will affect it. Global atmospheric circulation is likely to change as is the EASM. Climate change will not only affect the regional climate and regional water resources (Ding et al., 2023); it will affect East Asia (dust storms) and even the rest of the globe. Hence the study of climate in this region is of great practical and theoretical significance (Chen et al., 2019a; Chen et al., 2019b).

The westerly winds and the EASM meet at the northern boundary of the Asian summer monsoon (Huang et al., 2023). In northern China, this boundary runs from west to east, along the eastern section of the Qilian Mountains, the southern foothills of the

71 Helan Mountains, the Daqing Mountains, and the western section of the Daxinganling

72 Mountains. This is not a static boundary. It fluctuates within a range of 200–700 km

73 (Chen et al., 2018). It is important to understand the history of these fluctuations (Huang

74 et al., 2023).

75 This can be done using climate records such as lacustrine, eolian, and

76 dendrochronological (Sun et al., 2003; Liu et al., 2005; Li, 2009; Chen et al., 2010; Li

77 et al., 2016; Chen et al., 2019b; Qin et al., 2023). Our research team specializes in

78 dendrochronology, which is one of the best tools for studying paleoclimatic changes,

79 due to its precise dating, high resolution, good continuity and high replication (Zhang

80 et al., 2003; Shao et al., 2010; Yang et al., 2014; Liu et al., 2016).

81

82 **1.2 Previous work**

83 The climate history of the Baotou area, at the northern edge of the EASM, has been

84 studied at interannual and interdecadal scales for the past 260 years, based on June–

85 August precipitation reconstruction from tree-ring samples from the western Yinshan

86 Mountains (Liu et al., 2001; Liu et al., 2003). Using tree-rings and historical records,

87 Kang and Yang (2015) reconstructed the annual precipitation history of the East Asian

88 monsoon northern fringe zone for the last 530 years. They analyzed spatial variability

89 and possible driving mechanisms using the 400-mm isohyet.

90 Several May–July precipitation sequences have been reconstructed using ring-

91 width and latewood-width data from Chinese pine (*Pinus tabulaeformis*) growing in

92 the Helan Mountains (Ma et al., 2003; Liu et al., 2004; Chen et al., 2016). Studies of

93 tree-ring carbon and oxygen isotopes from Chinese pine samples have shown that $\delta^{18}O$

94 values increase with summer precipitation, while $\delta^{13}C$ values decrease (Zhang et al.,

95 2005a; Liu et al., 2008). Westerly winds have also been shown to affect precipitation in

96 the Helan Mountains (Chen et al., 2010).

97 Principal component analysis of tree-ring chronologies constructed from data

98 collected at several sites in Gansu suggests that trees at these sites were more influenced

99 by EASM than by west winds (Chen et al., 2013). These researchers also found that the

100 EASM weakened in 1970s, but recovered in the early 1990s. Tree-ring data allowed the

101 reconstruction of 330 years of PDSI values for the Mount Hasi region (at the northern

102 boundary of the summer monsoon zone) (Kang et al., 2012). This study confirmed that

103 radial growth of Chinese pine has declined over the past three decades, due to the

104 weakening of the EASM. Dendrochronological reconstruction of precipitation in the

105 Mount Changling region (again using Chinese pine) suggested that precipitation in that

106 region mainly depends on the EASM (Chen et al. 2012). Other researchers have

107 assembled tree-ring chronologies from pines growing in the Mount Qilian region and

108 the northern mountains of the Hexi Corridor. Here again precipitation is associated with

109 the EASM. These chronologies have allowed scholars to compile precipitation,

110 temperature, and drought records for the last thousand years (Gou et al., 2015a; Gou et

111 al., 2015b; Zhang et al., 2017).

112 Most modern researchers studying climate change in the region are mostly carried

113 out on single sample sites (Wang et al., 2004; Liu et al., 2005; Chen et al., 2010; Chen

114 et al., 2016; Li et al., 2016; Liu et al., 2016; Chen et al., 2018). There is a dearth of

115 multi-site, regional, large-scale studies on the interaction of the westerlies and the

116 EASM. Our group compiled and analyzed tree-ring chronologies from Qinghai spruce

117 (*Picea crassifolia*) growing in the Helan, Changling, and Dongdashan mountain regions

118 that surround the Alxa Plateau, the climate response characteristics of spruce radial

119 growth in three regions was then analyzed. Combining the relevant Westerly and East

120 Asia monsoon circulation indices, the driving mechanism of the regional climate

121 change by with the interaction and synergistic roles of two atmospheric circulation

122 systems in the Alxa Plateau was explored. The results will lay a theoretical foundation

123 for the climatic evolution of the region and the desertification control.

124

125 **2. Material and methods**

126 **2.1 Study area**

127 The Alxa Plateau is located in the western part of the Inner Mongolia Autonomous

128 Region and is surrounded by mountains (Fig.1). It consists primarily of three deserts:

129 Tengger, Ulan Buh, and Badan Jaran. It lies south of the Gobi desert. It is the main

130 source of the fierce sandstorms and dust storms that blow toward eastern China and the

131 Pacific. It has been much affected by climate change; sand- and dust storms have

132 increased, much to the detriment of lands to the east. The Chinese government is doing

133 what it can to establish an environmental defense line there. It is currently the Northern

134 Sand Prevention Belt of the National Two Ecological Barrier and Three Belts

135 Ecological Security Strategy Pattern (Xiao et al., 2017; Xiao et al., 2019).
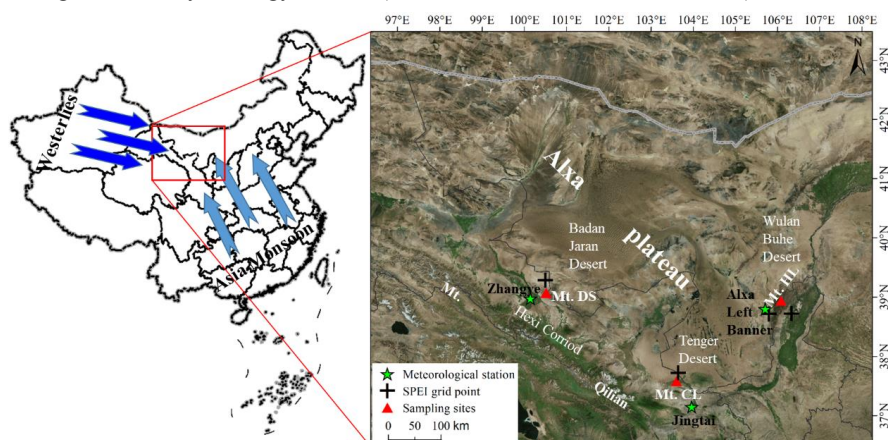
137 Figure 1. Location of tree-ring sampling sites and meteorological stations (the right

138 panel is from Mapworld)

139 There are several mountain ranges surrounding the Alxa Desert, such as the Helan

140 Mountains in the east, the northern mountains of the Hexi Corridor, and the outliers of

141 the Altai Mountains in the north. These mountains not only block the eastward and

142 southward expansion of the desert (driven by high pressure regions from Mongolia);

143 they are also the source of mountain rivers and streams that water the oases on the

144 plateau.

145 The Alxa Plateau is located in the eastern margin of the inland arid region of Central

146 Asia. It is affected not only by the mid-latitude westerly circulation, but also by the

147 Asian monsoon and the plateau monsoon. It is in the zone where the mid-latitude

148 westerly circulation and the Asian monsoon interact (Xiao et al., 2017; Chen et al.,

149 2019b). As a result, there is large interannual variability of vegetation cover in the

150 region (Ou and Qian, 2006; Tang et al., 2006; Li et al., 2013).

151 The Helan Mountains (38°27′~ 39°30′N, 105°20′~106°41′E) (sampling site

152 henceforth abbreviated as HL), are located at the eastern edge of the Tengger Desert.

153   They stretch more than 200 kilometers from north to south; the main peak is ~3,556 m.

154   The mountain forests are dominated by Qinghai spruce and Chinese pine, juniper,

155   mountain aspen, and elm.

156   Mount Changling (37°12′~37°17′, 102°45′~103°48′E) (sampling site henceforth

157   abbreviated as CL) is an independent mountain protruding northward from the

158   remnants of the eastern Qilian Mountains, It is located at the southern edge of the

159   Tengger Desert; its elevations range from 2100 to 2900 m. The dominant tree species

160   are Qinghai spruce and Chinese pine.

161   Mount Dongdashan (39°00′~39°04′N, 100°45′~100°51′E) (sampling site

162   henceforth abbreviated as DS) is located at the southwestern edge of the Badan Jaran

163   Desert and the middle part of Mount Qilian. It is one of the northern mountains along

164   the Hexi Corridor; that range consists of mountains that vary from 2200 to 2637 m in

165   elevation. Forests are dominated by Qinghai spruce and Qilian juniper.

166   The temperatures of the coldest months recorded at meteorological stations in the

167   Alxa Left Banner (a division of the Alxa League region), Jingtai (a county in Gansu),

168   and Zhangye (a city in Gansu) all occurred in January, ranging from -9.8℃ to -6.8℃.

169   The hottest months at those stations were in July (21.9 ℃ to 23.1 ℃). These

170   meteorological stations are the closest stations to our three sampling sites.

171   Precipitation measured at those stations varied widely. The multi-year average of

172   total precipitation from May to September was 171 mm at Alxa Left Banner station,

173   156 mm at Jingtai station, and 108 mm at Zhangye station. This accounted for more

174   than 80% of the annual precipitation (Fig.2).

Climate
of the Past
Discussions
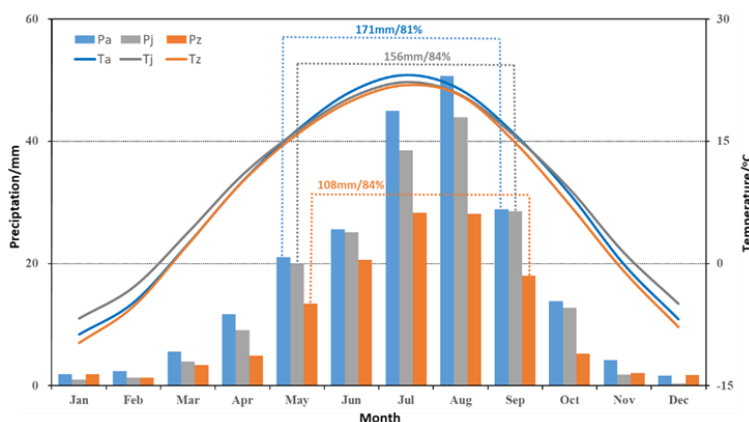
Figure 2. Climatic diagram of study area. Pa/Ta are the monthly total precipitation and monthly mean temperature at the Alxa Left Banner meteorological station (1953–2016); Pj/Tj are the precipitation and temperature figures for the Jingtai meteorological station (1957–2017); Pz/Tz are the precipitation and temperature figures for the Zhangye meteorological station (1957–2017). The dashed box and appended data indicate the total growing season precipitation in the study area and the proportion of total annual precipitation.

2.2 Sample collection, processing and data analysis method

2.2.1 Sample collection, processing and dendrochronology construction

Researchers used standard methods of tree-ring sample collection. One core was drilled from each tree in the sample site. We collected 209 cores in total, from five sampling sites at HL, 48 cores from one sampling site at CL, and 81 cores from two sampling sites at DS. Relevant information re the sampling sites is summarized in Table 1.

Chronologies were constructed using standard dendrochronological methods. We calculated the highly significant correlations (P<0.001) between the chronologies of different points at the HL and DS mountains; a weighting method was used to finally synthesize a chronology for each mountain.

2.2.2 Climate data, atmospheric circulation indices and the related Analyzing methods for chronological correlation

197   Climate data for the study areas HL, CL, and DS were collected from the nearest

198   meteorological stations in Alxa Left Banner, Jingtai and Zhangye, respectively

199   (http://data.cma.cn).

200   We used SPEI to represent the local drought and wetness conditions. SPEI data

201   (grid-point resolution 0.5º∗0.5 º) was obtained from the grid-point datasets of the

202   National Center for Environmental Predictions-National Center for Atmospheric

203   Research (NCEP-NCAR). Time scales ranged from 1 month to 15 months. The mean

204   values of data from two grid-points closest to the HL sampling site (38.75°N,105.75°E

205   and 38.75°N,106.25°E; period 1953–2015) were chosen for subsequent analysis. Grid-

206   point data from one site closest to our CL sampling site (37.75N, 103.75E; period 1951–

207   2015) was used for later analysis. Grid-point data from one site closest to our DS

208   sampling site (39.25°N, 100.75°E; period 1951–2015) was also used. As SPEI datasets

209   are multi-scale, we preprocessed the data to identify and select 11-month scaled SPEI

210   datasets for subsequent analysis.

211   We took into account the so-called lagging effect (the influence of fall and winter

212   climate factors on the radial growth of trees shows up later in the year) and chose to use

213   temperature, precipitation, and SPEI data from September of the previous year to

214   September of the current year (abbreviated as P9–P12 and C1–C9), as collected at each

215   meteorological station, for our climate response analysis.

216   The East Asian Summer Monsoon Index (EASMI) represents the activity strength

217   of the EASM. Larger EASMI values indicate a stronger summer monsoon, smaller ones

218   a weaker monsoon. In this study, the EASMI (mean values for June–August in the

219   period 1950–2017) defined by Li and Zeng (2005) was used to study the impact of the

220   EASM on climate change in the study area.

221   We used the Westerly Circulation Index (WCI annual mean) to represent the

222   strength of the mid-latitude westerlies. The larger the WCI value, the stronger the

223   Eurasian latitudinal circulation; the smaller the value, the weaker the Eurasian

224   latitudinal circulation. WCI data (period 1951–2015) were derived from the Eurasian

225   Latitudinal Circulation Index published by the National Climate Center of the China

226   Meteorological Administration (https://cmdp.ncc-cma.net/cn/index.htm).

227   Interannual and interdecadal (sliding moving average of 11a) chrono-climatic/-

228   cyclonic index correlation and partial correlation analyses were performed using SPSS

229   19.0. Based on the characteristics of tree-ring series, the sequences were classified into

230   three groups of low, average and high ring widths using mean $\pm$ 1δ (SD) as the

231   classification criterion (with mean $\pm$ 2δ as the extreme year). Correlation statistical tests

232   were performed with the corresponding annual circulation indices; similar treatments

233   and analyses were performed for the two major circulation indices.

234

235

236   **3. Results and analysis**

237   **3.1 Ring-width chronologies and their characteristics**

238   Based on the sampling cores from five sample sites at HL, two sample sites at DS, and

239   one sample site at CL, ring-width residual chronologies were derived for each of the

240   three study areas (Fig. 3). Statistical parameters showed that the three chronologies

241   meet the usual requirements for correctly done dendrochronological studies. (Table 1).

242
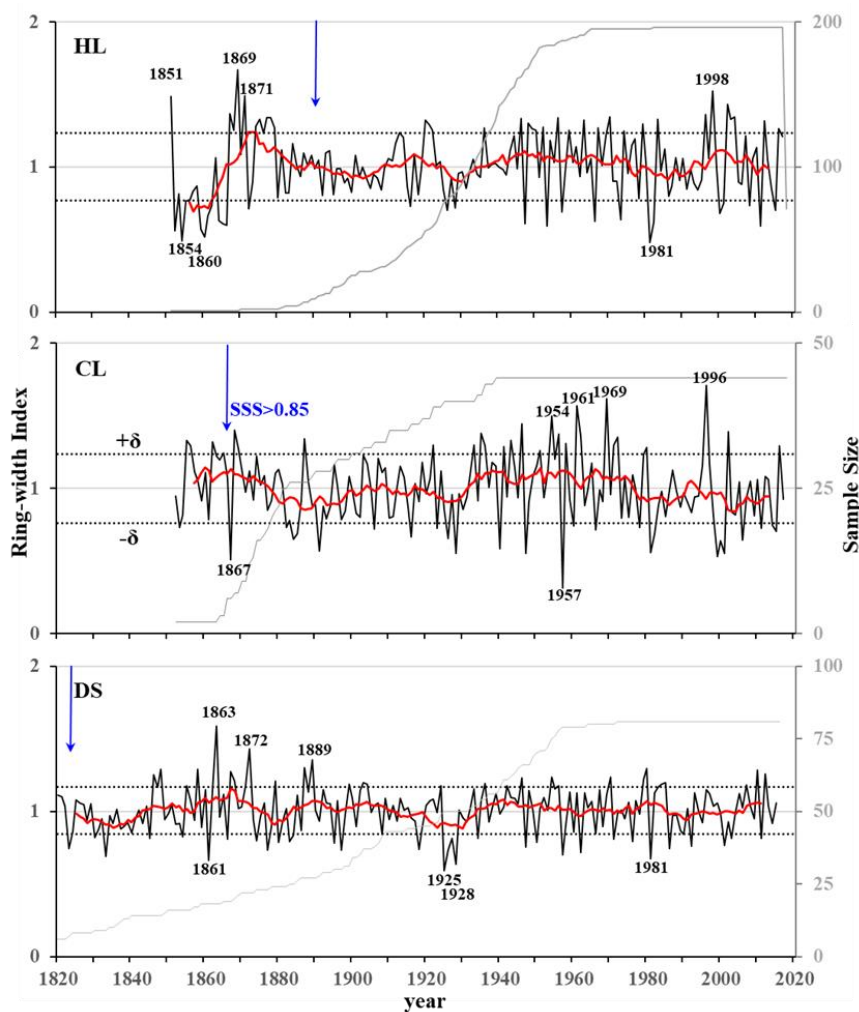
Figure 3. Residual ring-width chronologies for the three study areas. The dark lines indicate the chronology; grey lines indicate the sample depth; red lines indicate the 11-year running mean chronology; dotted horizontal lines indicate the mean value +/-1δ, years with data identified as >/< mean +/-2δ (δ: standard deviation); the blue arrows indicate the start of the reliable residual chronology (SSS>0.85).

Table 1. Statistical characteristics of the sampling sites and the tree-ring chronologies.

Sampling sites	HL(5)	CL(1)	DS(2)
Latitude (°N)	38.52–38.97	37.61	39.04
Longitude (°E)	105.83–106.02	103.71	100.78

Elevation (m)	2200–2750	2490	2650–2700
Cores	209	48	81
Reliable period	1891–2018	1866–2017	1823–2015
MS	0.18–0.37	0.28	0.15–0.33
Rbar	0.45–0.61	0.56	0.40–0.60
SNR	22.5–56.1	38.9	25.7–42.5
EPS	0.96–0.98	0.98	0.96–0.98
PC1(%)	17.3–63.0	57.9	43.0–62.5

249 Reliable period, MS (mean sensitivity), Rbar (mean series intercorrelation), SNR (signal to noise ratio),

250 EPS (expressed population signal), and PC1 (variance explained by the first principal component) refer

251 to residual chronologies.

252

3.2 Climate response characteristics

254 Correlation analysis comparing a) monthly mean temperature and precipitation at

255 neighboring meteorological stations and b) SPEI at the nearest grid-point showed that,

256 overall, the three residual chronologies were correlated negatively with monthly mean

257 air temperature, positively correlated with monthly precipitation, and positively

258 correlated with SPEI during the growing season (Fig. 4).
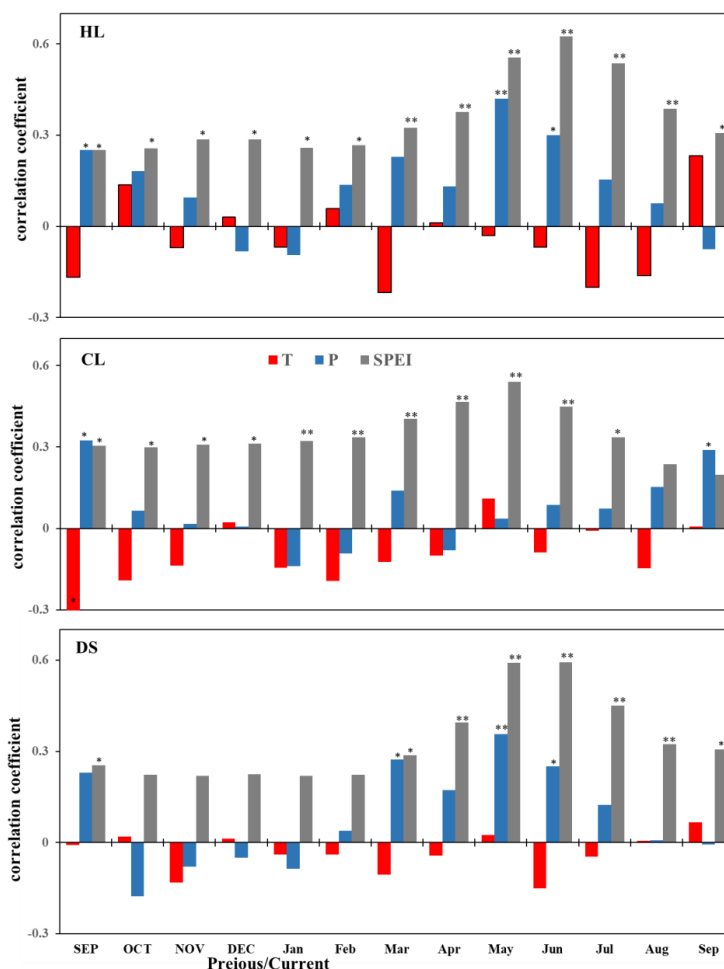
Figure 4. Correlation coefficients (Pearson's r values) between the residual ring-width chronologies of Qinghai spruce at the three study areas (HL, CL and DS) and the observed monthly temperature (T), total monthly precipitation (P), and SPEI.

 * Pearson's r correlation, significant at P < 0.05.

 * * Pearson's r correlation, significant at P < 0.01.

 Month names of previous year are capitalized.

     HL chronology was correlated negatively with mean temperature mainly in C5–C8 in the growing season, but not to the significant level. It was also positively correlated with precipitation in all months except P12, C1, and C9, reaching significant levels (P<0.05) in P9, C5, and C6. All months were positively correlated with SPEI and

270 reached statistical significance (P<0.05), with C3–C8 showing highly significant

271 correlation levels (P<0.01).

272   CL chronology was negatively correlated with mean temperature in all months

273 except for P12, C5 and C9. Only P9 reached statistical significance (P<0.05). CL

274 chronology was positively correlated with monthly precipitation, save for C1, C2, and

275 C4. Only P9 and C9 reached statistical significance (P<0.05). All months were

276 positively correlated with SPEI, with P9–C7 reaching significant correlation levels

277 (P<0.05) and C1–C7 reaching highly significant correlation levels (P<0.01).

278   DS chronology showed weak correlations between DS chronology and monthly

279 mean temperatures. None of the correlations reached levels of significance. DS

280 chronology was positively correlated with P9 and C2-C8 precipitation and reached

281 significant correlation levels for C3, C5, and C6 (P<0.05). All months were positively

282 correlated with SPEI, with P9 and C3-C9 reaching significant correlation levels

283 (P<0.05) and C4-C8 reaching highly significant correlation levels (P<0.01).

284   Overall, the radial growth of Qinghai spruce at the three study areas seems to have

285 been limited, for the most part, by low precipitation during the growing season (April–

286 July). The three chronologies reflect regional wet and dry variations.

287

288 3.3 Regional climate changes as recorded by tree-ring widths

289 3.3.1 Regional climate change viewed at interannual scales

290 On interannual scales, the three residual chronologies, when compare, showed highly

291 significant correlations. HL-CL: n=166 (P<0.01); HL-DS: n=165 (P<0.01); CL-DS:

292 n=164, P<0.01). This indicates that there was a high degree of consistency in the radial

293 growth of Qinghai spruce in the three regions.

294   According to the results of the chronology-climate response analysis in the

295 previous section, the high and low ring-width indices (mean±1~2δ) of the chronology

296 at the three sample sites indicate wetter or drier, and extreme wet or dry years,

297 respectively (Table 2).

298   Overall, the three ring-width residual chronologies (HL, CL, DS) had a total of two

299 shared wetter years and seven shared drier years. The HL and CL chronologies shared

300 four wet years and eleven dry years; the HL and DS chronologies shared five wet years

301 and nine dry years; and the CL and DS chronologies shared five wet years and seven

302 dry years (Table 2).

303   Table 2. Years of high or low growth, wet or dry climate in the three chronologies

chronology	Higher index/wetness years (≥mean+1δ)	Lower index/drought years (≤mean-1δ)
HL	**1851**, 1867, **1869**, **1871**, 1874, 1875, 1877, 1878, 1879, 1920, 1921, 1922, 1936, 1946, 1952, 1959, 1963, 1967, 1970, 1974, 1979, 1983, 1996, **1998**, 2002, 2003, 2004, 2012, 2016	1852, **1854**, 1855, 1859, **1860**, 1861, 1864, 1865, 1866, 1872, 1916, 1926, 1928, 1947, 1953, 1957, 1966, 1973, **1981**, 1982, 2000, 2001, 2011
CL	1855, 1862, 1922, 1933, 1935, 1936, 1941, 1946, 1951, **1954**, 1958, **1961**, **1969**, 1972, 1980, **1996**, 2016	**1867**, 1884, 1885, 1891, 1916, 1923, 1926, 1928, 1947, **1957**, 1960, 1966, 1978, 1981, 1982, 1999, 2000, 2001, 2006, 2011, 2014, 2015
DS	1846, 1848, 1855, 1858, **1863**, 1867, 1868, **1872**, 1879, 1887, **1889**, 1899, 1903, 1904, 1924, 1936, 1942, 1946, 1954, 1956, 1959, 1970, 1979, 1980, 2007, 2010, 2012	1823, 1830, 1833, 1854, **1861**, 1874, 1877, 1880, 1883, 1884, 1895, 1897, 1908, **1925**, 1926, 1927, **1928**, 1934, 1947, 1950, 1957, 1962, 1971, 1976, **1981**, 1985, 1990, 1992, 2001, 2003, 2011

304 Note: Bold is used to indicate extreme years (>/<mean+/-2δ ; δ : standard deviation); double

305 underlining indicates years shared between two of the three sample sites; bold underlining

306 shows years shared between three sample sites.

307   There were no extremely wet years shared by the three sample sites. However, there

308 were two shared wetter years in 1936 and 1946 and several shared wetter years in later

309 years among the three sample sites. For example, note the wetter years in 1922 and

310 2016 for HL and DS chronologies; 1959, 1979, and 2012 for HL and DS chronologies;

311 1855, 1954, and 1980 for CL and DS chronologies (Table 2).

312   The extreme drought years are consistent among the three sample sites. For

313 instance, there was an extreme drought year in 1981 at HL and DS sample sites; it was

314 also a drought year at CL. An extreme drought year at CL in 1957 was also a drought

315 year for the other two chronologies. Moreover, the extreme drought year of 1928 at DS

316 was a drought year at the other two sites. Drought years in 1926, 1947, 2001, and 2011

317   were seen in all three sites and in two of the three sample sites (1916, 1966, 1982, and

318   2000 at HL and CL; 1854 and 1861 at HL and DS) (Table 2).

319

320   **3.3.2 Characteristics of regional climate change at inter-decadal scales**

321   On the decadal scale, the 11a running mean series indicates that at the HL site there

322   were four wetter periods (mid-1860s to early 1880s; 1910s to 1920s; mid-1930s to mid-

323   1970s; and late 1990s to early 2010s). Four drought periods were seen (mid-1850s to

324   mid-1860s; early 1890s to late 1900s; circa 1930s; and mid-1970s to 1980s) (Fig.5).
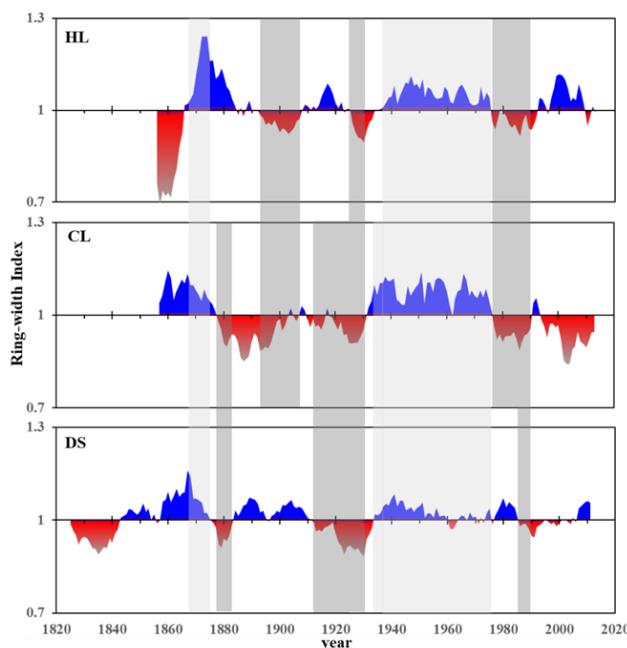
325

326   Figure 5. Three regional chronologies demonstrating alternation between dry and wet

327   years on interdecadal scales (11 a running mean). The gray bands indicate consistent

328   changes.

329   The CL regional chronology revealed two main wetter periods (mid-1850s to mid-

330   1870s; mid-1930s to mid-1970s) and two longer drought periods (late 1870s to early

331   1930s; following the late 1970s) (Fig.5).

332   The DS regional chronology showed four main wetter periods (mid-1840s to mid-

333   1870s; mid-1880s to late 1900s; mid-1930s to mid-1980s; and late 2000s to early

334 2010s). There were four drought periods (mid-1820s to mid-1840s; mid-1870s to 1880s;

335 early 1910s to early 1930s; and late 1980s to mid-2000s). The drought during the last

336 drought period was less severe (Fig.5).

337   The three chronologies show both synchronized phases and differential changes on

338 an interdecadal scale. The more synchronized dry phases of climate change were the

339 drought periods of the 1930s and 1990s. When we compared the DS chronology to the

340 HL and CL chronologies on decadal scales, we noted that DS droughts tended to last

341 longer and that they started and ended later than CL droughts. However, HL and DS

342 droughts tended to end at close to the same time (Fig.5).

343   There were two wet periods in 1870s and the mid-1930s to 1970s which were

344 shared by all three sample sites. The latter period was the longest lasting wet period we

345 saw in our study. There were also dry and wet periods that were not shared by any of

346 our sites. There was an HL drought (mid-1850s to mid-1860s) which was not shared by

347 the other two sites, which were wetter. HL and CL shared drought periods (1890s to

348 1910s; 1980s) while DS was wetter. Conversely wetter periods at HL were sometimes

349 accompanied by drought in the other two sites. Drought at CL was sometimes

350 accompanied by wet periods at the other two sites. DS was wet during the 2010s but

351 the other two sites were in drought (Fig.5).

352   The results of the above studies show that there are diversified and complex

353 features in the interdecadal processes of climate change in different regions around the

354 Alxa Plateau.

355

356 **3.4 Driving mechanism of the regional climate changes**

357 **3.4.1 Driving mechanism of the regional climate changes of typical years**

358   On the interannual scales, three regional chronologies we developed showed fairly

359 weak negative correlations between the EASM and the westerlies; none of the

360 correlations were statistically significant. We carried out correlation analyses of the

361 three regional ring-width chronologies and two major circulation indices. This was

362 done in high, medium and low ring-width index groups (Fig. 6; 7).

363   At HL, the results of our combined subgroup correlation analyses suggest that

364   correlations between radial growth groups and atmospheric circulations were stable.

365   Correlation between the higher ring-width group and atmosphere circulation indices

366   and between the lower ring-width group and the WCI were all significant (P<0.05) (Fig.

367   6; 7).

368   At CL, correlations between the higher and middle ring-width groups to the WCI

369   and the higher and middle WCI groups to the ring-width index were all negative.

370   Correlations between the higher and middle ring-width groups and the EASMI, and

371   between the higher and middle EASMI groups with the ring-width index were

372   inconsistent (Fig. 6; 7).

373   At DS, correlations between the higher and lower ring-width groups and the

374   EASMI, and between the higher and lower EASMI groups to the ring-width indices,

375   were consistent. The correlations between the higher ring-width groups and the WCI,

376   and between the higher WCI groups and the ring-width index were consistent. However,

377   the correlations between the lower ring-width groups and the WCI, also between the

378   lower WCI groups and the ring-width index, were inconsistent (Fig. 6; 7).
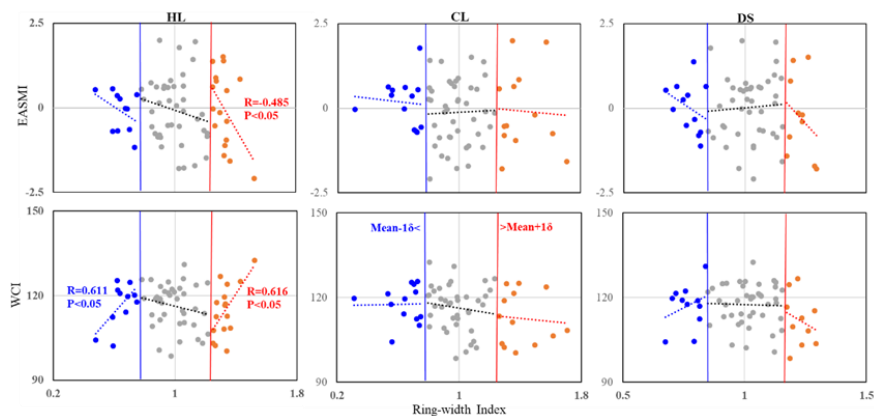
379

380   Figure 6. Grouping related charts among the ring-width index of three regions (HL, CL

381   and DS) and the two atmospheric circulations' indices (EASMI and WCI). The noted

382   numbers are the person correlation coefficients (two-tails test) and the corresponding

383   significant credible level. Red dots indicate the higher ring-width index group

384   (>mean+1δ), gray dots indicate the middle ring-width index group (>mean-1δ~<

385   mean+1δ), and blue dots indicate the lower ring-width index group (>mean-1δ).
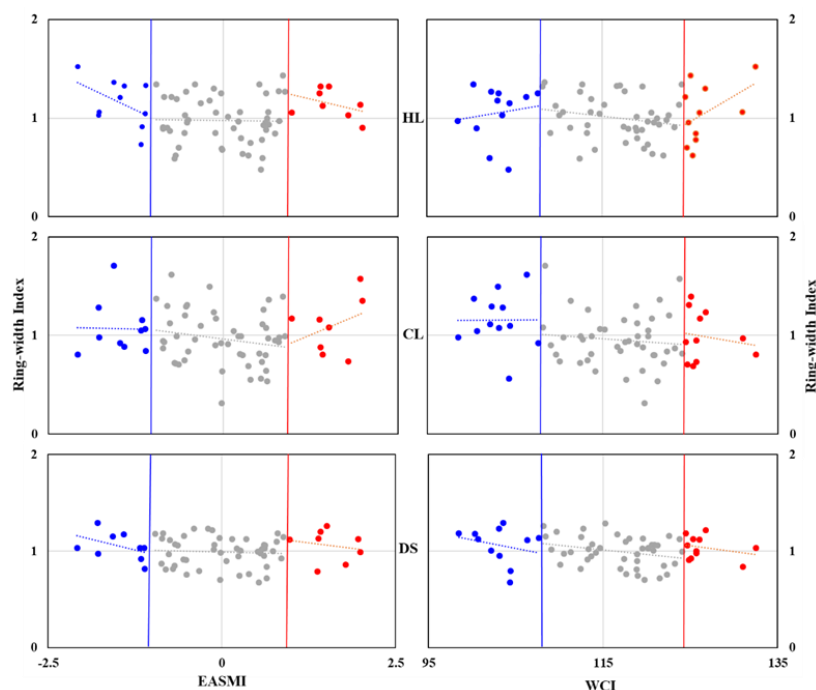
386

387   Figure 7. Grouping related charts among the two atmosphere circulations' index

388   (EASMI and WCI) and the ring-width index of three regions (HL, CL, and DS). Red

389   dots indicate the higher atmosphere circulations' index group (>mean+1δ), gray dots

390   indicate the middle atmosphere circulations' index group (>mean-1δ~< mean+1δ), and

391   blue dots indicate the lower atmosphere circulations' index group (>mean-1δ).

392   Except for HL, none of the ring-width groups or the atmospheric circulation index

393   groups of the others reached a level of significance. These results suggest that HL is

394   strongly affected by size of, and the interaction between, the EASM and the westerlies.

395   On an interannual scale, stronger west winds and a weaker monsoon could result in

396   variations from the ordinary climate (veering towards drier or wetter). Weaker west

397   winds and a stronger monsoon formed the normal climate at HL. At the CL and DS

398   sites, both atmospheric circulations were relatively weak on interannual scales. They

399   had complex interactions.

400

3.4.2 Driving mechanisms of the regional climate changes on a decadal scale

At HL, both the EASM and the westerly circulation had highly significant effects on the radial growth of the Qinghai spruce. At CL, the EASM also had highly significant effects on radial growth of the Qinghai spruce. There, correlation coefficients were higher for the EASMI (EASM index) than they were for the HL index. Correlations between the WCI and radial growth were negative, but not at a significant level.

At DS, correlation between radial growth and the WCI was extremely negative ($P<0.01$). Correlation between radial growth and the EASM was positive ($P>0.1$) (Fig. 8). These results suggest that at HL, alternations between dry and wet seasons were affected both by the EASM and the westerlies. If either of the two atmospheric circulations was stronger, the climate tended to be wetter. At CL, alternations between dry and wet were affected mainly by the EASM. When the EASM was stronger, the climate was wetter. At DS, the climate was affected mainly by the westerly winds. The stronger the winds, the wetter the climate (Fig. 8).
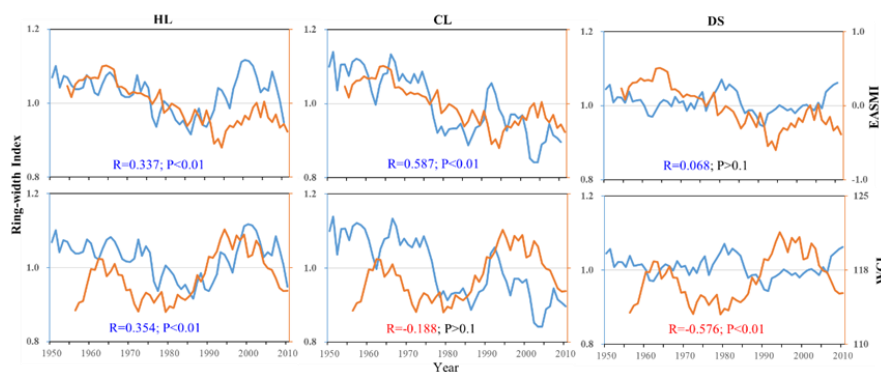
Figure 8. Interdecadal scale (11-a running average) correlations of the three residual chronologies with the EASMI and WCI.

The results of our interdecadal partial correlation analysis of the three RES-chronologies with the WCI and EASMI further illustrate the impacts of the two circulation systems on the climate of the three regions (Table 3).

At HL, if we control one factor (the WCI or EASMI) from our analysis, the other factor showed a positive correlation ($P<0.0001$). At CL, if we controlled the WCI, we find a positive significant correction with EASMI ($P<0.0001$). If we controlled the

424 effect of EASMI, we saw a weak negative correction with WCI (Table 3). At DS, if we

425 controlled EASMI, we saw a negative significant correlation with WCI (P<0.0001). If

426 we controlled the WCI, we saw an insignificant negative correlation with EASMI

427 (Table 3).

428 Table 3. Inter-decadal partial correlation analysis of the three residual-chronologies

429 with the WCI and EASMI.

	HL	CL	DS
WCI	0.489***	0.550***	-0.172
EASMI	0.511***	-0.001	-0.591***

430 Correlation significance levels (two-tailed test): *** P < 0.001.

431 Summary: at HL (on the eastern boundary of the Alxa Plateau), both EASMI and

432 WCI influenced the alternation between wet and dry; at CL (on the southern boundary

433 of the Alxa Plateau), climate was mainly influenced by the EASM. At DS (on the

434 western boundary of the Alxa Plateau and the middle part of Hexi Corridor), climate

435 was mainly influenced by the westerly winds.

436

437 **4. Discussion and conclusions**

438 **4.1 Climate changes indicated by regional chronologies**

439 Our chronology-climate response analysis (Fig. 4) showed that the radial growth index

440 of Qinghai spruce in the HL, CL and DS mountains were a good record of regional

441 climate changes around the Alxa Plateau (Fig. 3). On the interannual scale, the three

442 regional chronologies noted that the extreme drought years of 1928, 1957 and 1981

443 were shared by two or more locations, as were the drought years of 1854, 1861, 1916,

444 1926, 1947, 1966, and 2001 (Fig. 3 and Table 3).

445 We note that drought was also reported by other tree-ring studies for these regions

446 (Chen et al., 2016), also for the Qilian Mountains (Zhang et al., 2011; Zhang et al.,

447 2017). Several other drought years (1854, 1884, and 1925–1928) were also seen in the

448 dry-wet climate history (PDSI) (recorded by tree-ring-widths) in the nearby area of

449 Mount Hasi, which lies on the edge of the regions most influenced by the EASM (Kang

450 et al., 2012).

451   The drought years of 1823, 1833, 1854, 1877, 1883–1885, 1895, 1908, 1971, 1992,

452 and 2003 seen in results for the Alxa Plateau are also seen in twelve tree-ring

453 reconstructed drought series for the Qilian Mountains (an area mainly influenced by

454 westerly winds) (Zhang et al., 2011). We also note that wetter years seen in our three

455 regional chronologies were also seen in results from the Hasi and Xinglong Mountains,

456 which are also on the edge of the area influenced by the EASM) (Fang et al., 2009;

457 Kang et al., 2012).

458   If we compare our results with those seen for the EASM-affected areas at Mount

459 Guiqing, 1820–2005 (Fang et al., 2010), we noted that only three of the eight drought

460 years in that area (1928, 2000, and 2001) were seen in our three chronologies. We also

461 noted results from the westerly-influenced area at Mount Tianshan (Jiang et al., 2017).

462 The wetter years of 1846, 1903 and 1942 at DS were also extreme wet years at Mount

463 Tianshan. Two wet years, 1848 and 1959, recorded at DS are either one year earlier or

464 one year later than extremely wet years at Mount Tianshan, which might suggest some

465 correlation. Drier years at DS (1884, 1947 and 1951) are one or two years later than the

466 extremely dry years at Mount Tianshan. This suggests that these phenomena could be

467 related to broader changes in the extent and strength of the atmospheric circulation.

468   On a broader (interdecadal) scale, an extreme drought period in 1920s–1930s was

469 shared by much of northern China (Liang et al., 2006; Fang et al., 2009; Fang et al.,

470 2010). This is the same drought that we note our chronologies for HL, CL and DS (Liu

471 et al., 2002; Chen et al., 2010; Fan et al., 2012; Liu et al., 2013; Zhang et al., 2015). A

472 drought in 1890–1900 was noted by dendrochronological studies and regional history

473 documents (Yuan, 1994; Ma et al., 2003; Cai and Liu, 2007).

474   Ma and Fu's (2006) study showed a broad shift towards a drying climate in 1977–

475 78 (eastern area in northwestern China, also northern China). Several other

476 dendrochronological studies showed a combination of high temperatures and low

477 precipitation in the late 1970s to early 1990s (Zhang et al., 2005b; Cai and Liu, 2007;

478 Cai, 2009).

479   This same drought was seen at DS, if somewhat later and for a shorter time. We

480   also noted its effects at HL and CL. This would be   consistent with the increased

481   humidity of the climate in the eastern region of Northwest China (the EASM-influenced

482   region experiencing >400 mm precipitation). This region would include Mount

483   Xinglong (Fang et al., 2009; Chen et al. 2015), the easternmost part of the Qilian

484   Mountains, and Mount Guiqing (Fang et al., 2010).

485   The wet period that lasted from the 1940s to the early 1970s has been recorded by

486   several tree-ring-width chronologies covering HL, CL, and DS (Liu et al., 2004; Liu et

487   al., 2005; Gao et al., 2006; Cai, 2009; Chen et al., 2010). Regional history documents

488   also record some severe floods disasters in this period (Yuan, 1994). We also see this

489   wet period in tree-ring-width chronologies from Mount Xinglong (Fang et al., 2009;

490   Chen et al. 2015) and Mount Guiqing (Fang et al., 2010).

491   The wet period in the 1830s–1840s evident in the chronologies in Xinglong

492   Mountain (Fang et al., 2009)(Chen et al. 2015) and Guiqing Mountain (Fang et al., 2010)

493   corresponds to the dry period of DS. The wet period in the 1830s–1840s corresponds

494   to the dry period of HL and CL, and to the wet period of DS. The observed phenomena

495   can be attributed to differences in the extent and intensity of EASM and westerly

496   atmospheric circulations.

497

4.2 Influence of atmospheric circulations and their interaction on climate change
498

in the Alxa Plateau
499

500   It is known that that water vapor carried by the westerly winds will extend southward

501   to the northern part of Qinghai, the Hexi region of Gansu, the northern part of Ningxia,

502   and the northern part of Shaanxi Province, sometimes passing through the northern

503   border of the Xinjiang region (Li et al., 2012). The area bounded by 35° and 55°N,

504   110°E and 140°E seems to key to fluctuations in the westerly winds. This in turn affects

505   the distribution of rain belts in summer. Its mean WCI are weaker positively to the

506   rainfall in the middle of Yellow River Basin and its northern regions (Yan et al., 2007)..

507   The results showed that the middle ring-width index group of Qinghai spruce in the

508   three sample sites, which are located in the key area for interaction between wind and

509   monsoon, presented weaker negative correlation with WCI on the interannual scale (Fig.

510   6).

511   The EASM boundary zone has a greater influence on precipitation at higher

512   latitudes and thus on vegetation growth. This boundary zone can fluctuate due to the

513   interannual variability of the EASM and the westerlies. There may be lagging effects

514   at the mid-latitudes (Ou and Qian, 2006). Again, we note that on an interannual scale,

515   there is much variation in the strengths and interactions of the EASM and westerly

516   circulation and thus on climate in our three study regions (Fig. 6).

517   Sun et al. (2019) showed that when the westerly circulation strengthens, high

518   latitude air pressure drops across the entire Asian continent. Siberian high pressures and

519   the EASM are weakened. The south of the cold air activity is also correspondingly

520   weakened. That is not conducive to the north and south of the cold and warm air vapor

521   exchange to form precipitation. When the lower of the WCI and weakened latitudinal

522   circulation, the meridional circulation will strengthen, which favors the exchange of

523   warm and cold air between the north and south to form precipitation.

524   Yang et al. (2019) proposed that in years with weak summer westerlies in the

525   middle latitudes, the upper-level jet stream tends to shift southward. This southward

526   displacement of the jet stream, coupled with weakened lower-level divergence, hampers

527   the northward transport of warm air into the southwestern region. Consequently, this

528   leads to reduced availability of water vapor sources and ultimately results in diminished

529   summer precipitation within the transitional zone of typical monsoon activity. If the jet

530   stream moves northward, precipitation increases.

531   Xu et al. (2010) wrote that in the middle Qilian Mountains the westerly winds affect

532   precipitation directly, while the EASM only indirectly affects precipitation. When the

533   westerly winds are stronger, the high precipitation zone moves northwestward; when

534   they are weaker, the zone moves.

535   At DS, radial growth showed weak negative correlations with higher WCI and also

536   higher, middle, and lower EASMI groups (Figs. 6;7). At HL, when high chronology

537   indices are positive they are significantly correlated with westerly circulation; when

538   they are negative they significantly correlate with EASM (Figs. 6; 7). At CL, which lies

539   further to the south than HL, a higher EASMI leads to a more humid climate. Other

540   effects are more complicated: for example, the higher and lower ring-width index

541   groups, associated with extreme dry and wet climate years, have weak negative

542   correlations to EASMI (Figs. 6; 7). Jiang et al. (2019) published the results of their

543   hydrogen and oxygen isotope studies of surface water at more than 3,000 sampling sites

544   in northern China. They showed that surface water recharge in the DS Mountains is due

545   to the westerly winds; recharge in the CL Mountains is due to the EASM. The HL

546   Mountains, in contrast, sit at the boundary of the EASM; water recharge there is due to

547   both the EASM and the westerlies.

548   Jiang and Wang (2005) notes significant declines in the EASM in the mid-1960s

549   and mid-1970s, which led to decline in the radial growth of Qinghai spruce in our study

550   area. The effect of the latter declined period was much greater than that of the former,

551   whatever the intensity or duration. The effects of these declines were stronger at CL

552   and DS than at HL. In the mid-1970s, EASM retreat had stronger negative effects at

553   CL and then at HL. However, decline in the EASM proved to be a facilitator of radial

554   growth at DS (Fig. 8).

555   In the same period the westerly circulation also retreated. The EASM retreated

556   again in 1990s, while the westerly winds strengthened. This resulted in a drier climate

557   in the CL Mountains. However, it was also correlated with fluctuating wet periods at

558   HL and a weak wet period at DS. The above results, to a certain extent, support our

559   view on the driving mechanisms of climate change in the three study areas, especially

560   in the DS Mountains.

561   When we look at this area on a geologic scale, we learn that the westerly circulation

562   strengthened during the Ice Age. Westerly jet streams moved southward to about 35ºN.

563   When the westerly winds weakened in the Interglacial Age, the westerly jet streams

564   moved northward to ~37ºN (Sun et al., 2003). A study of Holocene lake level evolution

565   in the ancient Zhuye lake, central Alxa Plateau, showed that lake-level change was

566   subject to the combined effects of EASM and the arid climate of Central Asia (Li, 2009)

567   This result further illustrates the complexity of lake evolution and climate change in the

568   EASM marginal zone.

569   The westerly circulation also interacts with the monsoon on the Tibetan Plateau,
570   which has a profound effect on the climate of the Asian monsoon region as well as the
571   global climate (Qu et al., 2004). There has also been much research using proxy
572   indicator cycles indicating that our study area is also influenced by large-scale climate
573   and ocean-atmosphere changes on interannual and interdecadal scales, such as the
574   North Atlantic Oscillation (NAO), Pacific Decadal Oscillation (PDO), El Niño-
575   Southern Oscillation (ENSO), and sunspot activity (Gou et al., 2015a; 2015b; Liu et al.,
576   2016; Wang et al., 2017).

577   However, all of the above-mentioned large-scale climate and ocean-atmosphere
578   changes affect the EASM and westerly circulation through different pathways (Li.
579   2009), which in turn have various effects on the northwestern edge zone of the EASM
580   and the zone of interaction between the two major atmospheric circulations.

581   In conclusion, based on the analysis of the regional chronologies collected in the
582   HL, CL and DS mountains that are arrayed around the Alxa Plateau, we can safely assert
583   that the radial growth of Qinghai spruce in the study area is mainly affected by regional
584   precipitation. This precipitation varies constantly over time and space, primarily
585   influenced by the interactions between two atmospheric circulation systems, EASM
586   and westerly winds. At HL, both of these atmospheric circulation systems play a
587   significant role in shaping climate changes. At CL, the climate is mainly influenced by
588   the EASM. At DS, climate is more heavily influenced by the westerly circulation.

589   In the future, it is to be hoped that more refined, smaller scale research can be done
590   on the climate history in the deserts of the Alxa Plateau. Such research may finally to
591   provide a theoretical basis to explain   regional climate driving mechanisms and thus
592   enable better desertification controls.

593

594   **Competing interests:** The contact author has declared that none of the authors has any
595   competing interests.

596

597   **Acknowledgements**

The study was jointly funded by the National Natural Science Foundation of China (NSFC) (No.42171031; 42171167); Inner Mongolia Autonomous Region Special Fund project for transformation of Scientific and technological Achievements (2021CG0046).

References

Cai, Q. F.: Response of *Pinus tabulaeformis* tree-ring growth to three moisture indices and January to July Walter index reconstruction in Helan mountain, Marine geology & Quaternary geology, 29, 131–136 (In Chinese with English abstract), https://doi.org/10.3724/SP.J.1140.2009.06131, 2009.

Cai, Q. F. and Liu, Y.: January to August temperature variability since 1776 inferred from tree-ring width of *Pinus tabulaeformis* in Helan Mountain, Journal of Geographical Sciences, 17, 293–303, https://doi.org/10.1007/s11442-007-0293-5, 2007.

Chen, F., Yuan, Y. J., Zhang, T. W., and Linderholm, H. W.: Annual precipitation variation for the southern edge of the Gobi Desert (China) inferred from tree rings: linkages to climatic warming of twentieth century, Nat. Hazards, 81, 939–955, https://doi.org/10.1007/s11069-015-2113-z, 2016.

Chen, F., Wei, W. S., Yuan, Y. J., Yu, S. L., Shang, H. M., Zhang, T. W., Zhang, R. B., Wang, H. Q., and Qin, L.: Variation of annual precipitation during 1768-2006 in Gansu Inferred from multi-site tree-ring chronologies, Journal of Desert Research, 33, 1520–1526 (In Chinese with English abstract), https://doi.org/10.7522/j.issn.1000-694X.2013.00218., 2013.

Chen, F., Yuan, Y. J., Wei, W. S., Yu, S. L., Fan, Z. A., Zhang, R. B., Zhang, T. W., Li, Q., and Shang, H. M.: Temperature reconstruction from tree-ring maximum latewood density of Qinghai spruce in middle Hexi Corridor, China, Theoretical and Applied Climatology, 107, 633–643, https://doi.org/10.1007/s00704-011-0512-y, 2012.

Chen, F., Yuan, Y. J., Wei, W. S., Yu, S. L., Li, Y., Zhang, R., Fan, Z., Zhang, T., and Shang, H.: PDSI changes of May to July recorded by tree rings in the northern Helan Mountains, Advance in Climate Changes Research, 65, 344-348 (In Chinese with English abstract), 2010.

Chen, F. H., Chen, J. H., Huang, W., Chen, S. Q., Huang, X. Z., Jin, L. Y., Jia, J., Zhang, X. J., An, C., and Zhang, J.: Westerlies Asia and monsoonal Asia: spatiotemporal differences in climate change and possible mechanisms on decadal to sub-orbital timescales, Earth-Sci. Rev., 192, 337–354, https://doi.org/10.1016/j.earscirev.2019.03.005, 2019a.

Chen, F. H., Fu, B. J., Xia, J., Wu, D., Wu, S. H., Zhang, Y. L., Sun, H., Liu, Y., Fang, X. M., Qin, B. Q., Li, X., Zhang, T. J., Liu, B. Y., Dong, Z. B., Hou, S. G., Tian, L. D., Xu, B. Q., Dong, G. H., Zheng, J. Y., Yang, W., Wang, X., Li, Z. J., Wang, F., Hu, Z. B., Wang, J., Liu, J. B., Chen, J. H., Huang, W., Hou, J. Z., Cai, Q. F., Long, H., Jiang, M., Hu, Y. X., Feng, X. M., Mo, X. G., Yang, X. Y., Zhang, D. J., Wang, X. H., Yin, Y. H., and Liu, X. C.: Major advances in studies of the physical geography and living environment of China

636   during the past 70 years and future prospects, Science China Earth Sciences, 62, 1665–
637   1701, https://doi.org/10.1007/s11430-019-9522-7, 2019b.

638 Chen, J., Huang, W., Jin, L., Chen, J. H., Chen, S. Q., and Chen, F. H.: A climatological northern
639   boundary index for the East Asian summer monsoon and its interannual variability,
640   Science China Earth Sciences, 61, 13–22, https://doi.org/10.1007/s11430-017-9122-x,
641   2018.

642 Ding, Y. H., Liu, Y. J., Xu, Y., Wu, P., Xue, T., Wang, J., Shi, Y., Zhang, Y. X., Song, Y. F., and
643   Wang, P. L.: Regional responses to global climate change: progress and prospects for trend,
644   causes, and projection of climatic warming-wetting in Northwest China, Advances in
645   Earth   Science,   38,   551–562   (In   Chinese   with   English   abstract),
646   https://doi.org/10.11867/j.issn.1001-8166.2023.027, 2023.

647 Fan, Z. A., Wei, W. S., Chen, F., and Yuan, Y. J.: Precipitation variation from 1775 to 2005 at
648   the eastern margin of Tengger Desert, China inferred from tree-ring, Journal of Desert
649   Research, 32, 996–1002 (In Chinese with English abstract), 2012.

650 Fang, K. Y., Gou, X. H., Chen, F. H., D'arrigo, R., and Li, J. B.: Tree-ring based drought
651   reconstruction for the Guiqing Mountain (China): linkages to the Indian and Pacific
652   Oceans, Int. J. Climatol., 30, 1137–1145, https://doi.org/10.1002/joc.1974, 2010.

653 Fang, K. Y., Gou, X. H., Chen, F. H., Yang, M. X., Li, J. B., He, M. S., Zhang, Y., Tian, Q. H.,
654   and Peng, J. F.: Drought variations in the eastern part of northwest China over the past two
655   centuries: evidence   from   tree   rings,   Clim.   Res.,   38,   129–135,
656   https://doi.org/10.3354/cr00781, 2009.

657 Feng, W., Wang, K. L., and Jiang, H.: Influences of westerly wind inter-annual change on water
658   vapor transport over northwest china summer, Plateau Meteorology, 23, 270–275 (In
659   Chinese with English abstract), 2004.

660 Gao, S. Y., Lu, R. J., Qiang, M. R., Ha, S., Zhang, D. S., Chen, Y., and Xia, H.: Precipitation
661   variation recorded by tree-rings in the northern Tengger Desert of the last 140 years, Chin.
662   Sci. Bull., 51, 326–331, https://doi.org/10.1360/csb2006-51-3-326, 2006.

663 Gou, X. H., Gao, L. L., Deng, Y., Chen, F. H., Yang, M. X., and Still, C.: An 850‑year tree‑
664   ring‑based reconstruction of drought history in the western Qilian Mountains of
665   northwestern China, Int. J. Climatol., 35, 3308–3319, https://doi.org/10.1002/joc.4208,
666   2015a.

667 Gou, X. H., Deng, Y., Gao, L. L., Chen, F. H., Cook, E., Yang, M. M., and Zhang, F.: Millennium
668   tree-ring reconstruction of drought variability in the eastern Qilian Mountains, northwest
669   China, Climate Dynamics, 45, 1761–1770, https://doi.org/10.1007/s00382-014-2431-y,
670   2015b.

671 Huang, L. X., Chen, J., Yang, K., Yang, Y. J., Huang, W., Zhang, X., and Chen, F. H.: The
672   northern boundary of the Asian summer monsoon and division of westerlies and monsoon
673   regimes over the Tibetan Plateau in present-day, Science China Earth Sciences, 66, 882–
674   893, https://doi.org/10.1007/s11430-022-1086-1, 2023.

675 Jiang, D. B. and Wang, H. J.: Natural interdecadal weakening of East Asian summer monsoon
676   in the late 20th century, Chin. Sci. Bull., 50, 1923–1929, https://doi.org/10.1360/982005-
677   36, 2005.

678 Jiang, P., Liu, H. Y., Wu, X. C., and Wang, H. Y.: Tree-ring-based SPEI reconstruction in central
679   Tianshan Mountains of China since A.D. 1820 and links to westerly circulation, Int. J.
680   Climatol., 37, 2863–2872, https://doi.org/10.1002/joc.4884, 2017.

681 Jiang, W. J., Wang, G. C., Sheng, Y. Z., Shi, Z. M., and Zhang, H.: Isotopes in groundwater (^{2}H,
682   ^{18}O, ^{14}C) revealed the climate and groundwater recharge in the Northern China, Sci. Total
683   Environ., 666, 298–307, https://doi.org/10.1016/j.scitotenv.2019.02.245, 2019.

684 Kang, S. Y. and Yang, B.: Precipitation variability at the northern fringe of the Asian summer
685   monsoon in Northern China and its possible mechanism over the past 530 years,
686   Quaternary Sciences, 35, 1185–1193, https://doi.org/10.11928/j.issn.1001-
687   7410.2015.05.14, 2015.

688 Kang, S. Y., Yang, B., and Qin, C.: Recent tree-growth reduction in north central China as a
689   combined result of a weakened monsoon and atmospheric oscillations, Clim. Change, 115,
690   519–536, https://doi.org/10.1007/s10584-012-0440-6, 2012.

691 Li, D. L., Shao, P. C., and Wang, H.: The position variations of the north boundary of East Asia
692   subtropical summer monsoon in 1951-2009, Journal of Desert Research, 33, 1511–1519
693   (In Chinese with English abstract), https://doi.org/10.7522/j.issn.1000-694X.2013.00217,
694   2013.

695 Li, J. L., Li, Z. R., Yang, J. C., Shi, Y. Z., and Fu, J.: Analyses on spatial distribution and
696   temporal variation of atmosphere water vapor over northwest China in summer of later 10
697   years, Plateau Meteorology, 31, 1574–1581 (In Chinese with English abstract), 2012.

698 Li, J. P. and Zeng, Q. C.: A new monsoon index, its interauual variability and related with
699   monsoon precipitation, Climatic and Environmental Research, 10, 351–365 (In Chinese
700   with English abstract), 2005.

701 Li, W. L., Wang, K. L., Fu, S. M., and Jiang, H.: The interrelationship between regional Westerly
702   index and the water vapor budget in Northwest China, Journal of Glaciology and
703   Geocryology, 30, 28–34 (In Chinese with English abstract), 2008.

704 Li, Y.: The pollen records from lake sediments and climate & lake model in the Marginal area
705   of Asian monsoon, Lanzhou University, Lanzhou, China, 2009.

706 Li, Z. X., Feng, Q., Song, Y., Wang, Q. J., Yang, J., Li, Y. G., Li, J. G., and Guo, X. Y.: Stable
707   isotope composition of precipitation in the south and north slopes of Wushaoling Mountain,
708   northwestern China, Atmospheric Research, 182, 87–101,
709   https://doi.org/10.1016/j.atmosres.2016.07.023, 2016.

710 Liang, E. Y., Liu, X. H., Yuan, Y. J., Qin, N. S., Fang, X. Q., Huang, L., Zhu, H. F., Wang, L.,
711   and Shao, X. M.: The 1920s drought recorded by tree rings and historical documents in
712   the semi-arid and arid areas of Northern China, Clim. Change, 79, 403–432,
713   https://doi.org/10.1007/s10584-006-9082-x, 2006.

714 Liu, J. B., Chen, J., Chen, S. Q., Yan, X. W., Dong, H. R., and Chen, F. H.: Dust storms in
715   northern China and their significance for the concept of the Anthropocene, Science China
716   Earth Sciences, 65, 921–933, https://doi.org/10.1007/s11430-021-9889-8, 2022.

717 Liu, Y., Cai, Q. F., Ma, L. M., and An, Z. S.: Tree ring precipitation records from Baotou and
718   the East Asia summer monsoon variations for the last 254 years, Earth Sci. Front., 8, 91–
719   97 (In Chinese with English abstract), https://doi.org/10.3321/j.issn:1005-
720   2321.2001.01.012, 2001.

721 Liu, Y., Sun, C. F., Li, Q., and Cai, Q. F.: A *Picea crassifolia* tree-ring width-based temperature
722   reconstruction for the Mt. Dongda region, Northwest China, and its relationship to large-
723   scale   climate   forcing,   PLoS   One,   11,   e0160963,
724   https://doi.org/10.1371/journal.pone.0160963, 2016.

725 Liu, Y., Lei, Y., Sun, B., Song, H. M., and Li, Q.: Annual precipitation variability inferred from
726   tree-ring width chronologies in the Changling–Shoulu region, China, during AD 1853–
727   2007, Dendrochronologia, 31, 290–296, https://doi.org/10.1016/j.dendro.2013.02.001,
728   2013.

729 Liu, Y., Won-Kyu, P., Cai, Q. F., Jung-Wook, S., and Hyun-Sook, J.: Monsoonal precipitation
730   variation in the East Asia since A.D. 1840—tree-ring evidences from China and Korea,
731   Science   in   China   Series   D: Earth   Sciences,   46,   1031–1039,
732   https://doi.org/10.1007/BF02959398, 2003.

733 Liu, Y., Ma, L. M., Cai, Q. F., An, Z. S., Liu, W. G., and Gao, L. Y.: Reconstruction of summer
734   temperature (June-August) at Mt. Helan, China, from tree-ring stable carbon isotope
735   values since AD 1890, Science in China Series D: Earth Sciences, 45, 1127–1136,
736   https://doi.org/10.1360/02yd9109, 2002.

737 Liu, Y., Cai, Q. F., Liu, W. G., Yang, Y. K., Sun, J. Y., Song, H. M., and Li, X. X.: Monsoon
738   precipitation variation recorded by tree-ring δ^{18}O in arid Northwest China since AD 1878,
739   Chemical Geology, 252, 56–61, https://doi.org/10.1016/j.chemgeo.2008.01.024, 2008.

740 Liu, Y., Cai, Q. F., Shi, J. F., Hughes, M. K., Kutzbach, J. E., Liu, Z. Y., Ni, F. B., and An, Z. S.:
741   Seasonal precipitation in the south-central Helan Mountain region, China, reconstructed
742   from tree-ring width for the past 224 years, Canadian Journal of Forest Research, 35,
743   2403–2412, https://doi.org/10.1139/x05-168, 2005.

744 Liu, Y., Shi, J. F., Shishov, V., Vaganov, E., Yang, Y. K., Cai, Q. F., Sun, J. Y., Wang, L., and
745   Djanseitov, I.: Reconstruction of May–July precipitation in the north Helan Mountain,
746   Inner Mongolia since A.D. 1726 from tree-ring late-wood widths, Chin. Sci. Bull., 49,
747   405–409, https://doi.org/10.1007/BF02900325, 2004.

748 Ma, L. M., Liu, Y., Cai, Q. F., and An, Z. S.: The precipitation records from tree-ring late wood
749   width in the helan mountain, Marine geology ＆ Quaternary geology, 23, 109–114 (In
750   Chinese with English abstract), https://doi.org/10.16562/j.cnki.0256-1492.2003.04.016,
751   2003.

752 Ma, M. J., Pu, Z. X., Wang, S. G., and Zhang, Q. A.: Characteristics and numerical simulations

753   of extremely large atmospheric boundary-layer heights over an arid region in north-west
754   china, Boundary-Layer Meteorology, 140, 163–176, https://doi.org/10.1007/s10546-011-
755   9608-2, 2011.

756 Ma, Z. G. and Fu, C. B.: The basic facts of aridity in northern China from 1951 to 2004, Chin.
757   Sci. Bull., 51, 2429–2439 (In Chinese), https://doi.org/10.1360/csb2006-51-20-2429,
758   2006.

759 Ou, T. H. and Qian, W. H.: Vegetation variations along the monsoon boundary zone in East
760   Asia, Chinese Journal of Geophysics, 49, 698–705 (In Chinese with English abstract),
761   2006.

762 Qin, L., Liu, G. X., Li, X. Z., Chongyi, E., Li, J., Wu, C. R., Guan, X., and Wang, Y.: A 1000-
763   year hydroclimate record from the Asian summer monsoon-Westerlies transition zone in
764   the   northeastern   Qinghai-Tibetan   Plateau,   Clim.   Change,   176,   1–20,
765   https://doi.org/10.1007/s10584-023-03497-1, 2023.

766 Qu, W. J., Zhang, X. H., Wang, D., Shen, Z. X., Mei, F. M., Cheng, Y., and Yan, L. W.: The
767   important significance of westerly wind study, Marine Geology and Quaternary Geology,
768   24, 125–132 (In Chinese with English abstract), https://doi.org/10.16562/j.cnki.0256-
769   1492.2004.01.018, 2004.

770 Shao, X. M., Xu, Y., Yin, Z. Y., Liang, E. Y., Zhu, H. F., and Wang, S.: Climatic implications of
771   a 3585-year tree-ring width chronology from the northeastern Qinghai-Tibetan Plateau,
772   Quaternary   Science   Reviews,   29,   2111–2122,
773   https://doi.org/10.1016/j.quascirev.2010.05.005, 2010.

774 Sun, D. H., An, Z. S., Su, R. H., Deer, H. Y., and Sun, Y. B.: The dust deposition records of the
775   evaluation of Asia monsoon and Westerly circulation in north China in the last 2.6Ma,
776   Science in China (Series D), 33, 497–504 (In Chinese), 2003.

777 Sun, L. Q., Li, T. J., Li, Q. L., and Wu, Y. P.: Responses of autumn flood peak in the Yellow
778   River source regions to westerly circulation index, Journal of Glaciology and Geocryology,
779   41, 1475–1482 (In Chinese with English abstract), https://doi.org/10.7522/j.issn.1000-
780   0240.2019.0028, 2019.

781 Tang, X., Qian, W. H., and Liang, P.: Climatic features of boundary belt for East Asian Summer
782   Monsoon, Plateau Meteorology, 25, 375–381 (In Chinese with English abstract), 2006.

783 Wang, B. J., Huang, Y. X., He, J. H., and Wang, L. J.: Relation between vapour transportation
784   in the period of East Asian Summer Monsoon and drought in Northwest China., Plateau
785   Meteorology, 23, 912–917 (In Chinese with English abstract), 2004.

786 Wang, J. L., Yang, B., Ljungqvist, F. C., Luterbacher, J., Osborn, Timothy j., Briffa, K. R., and
787   Zorita, E.: Internal and external forcing of multidecadal Atlantic climate variability over
788   the past 1,200 years, Nature Geoscience, 10, 512–517, https://doi.org/10.1038/ngeo2962,
789   2017.

790 Wang, K. L., Jiang, H., and Zhao, H. Y.: Atmospheric water vapor transport from westerly and
791   monsoon over the Northwest China, Advances in Water Science, 16, 432–438 (In Chinese

792   with English abstract), https://doi.org/10.14042/j.cnki.32.1309.2005.03.021, 2005.

793 Xiao, S. C., Chen, X. H., and Ding, A. J.: Study process of climate changes, environment
794   evolution and its driving mechanism in the last two centuries in the Alxa Desert, Journal
795   of Desert Research, 37, 1102–1201 (In Chinese with English abstract),
796   10.7522/j.issn.1000-694x.2017.00002, 2017.

797 Xiao, S. C., Yan, C. Z., Tian, Y. Z., Si, J. H., Ding, A. J., Chen, X. H., Han, C., and Teng, Z. Y.:
798   Regionalization for desertification control and countermeasures in the Alxa Plateau, China,
799   Journal of Desert Research, 39, 182–192 (In Chinese with English abstract),
800   https://doi.org/10.7522/j.issn.1000-694X.2019.00068, 2019.

801 Xu, J. J., Wang, K. L., Jiang, H., Li, Z. G., Sun, J., Luo, X. P., and Zhu, Q. L.: A numerical
802   simulation of the effects of Westerly and Monsoon on precipitation in the Heihe River
803   Basin, Journal of Glaciology and Geocryology, 32, 489–496 (In Chinese with English
804   abstract), 2010.

805 Yan, H. S., Hu, J., Fan, K., and Zhang, Y. J.: The analysis of relationship between the variations
806   of Westerly Index in summer and precipitation during the flood period over China in the
807   last 50 years. , Chinese Journal of Atmospheric Science, 31, 717–726 (In Chinese with
808   English abstract), 2007.

809 Yang, B., Qin, C., Wang, J. L., He, M. H., Melvin, T. M., Osborn, T. J., and Briffa, K. R.: A
810   3,500-year tree-ring record of annual precipitation on the northeastern Tibetan Plateau,
811   Proc. Natl. Acad. Sci. USA, 111, 2903–2908, https://doi.org/10.1073/pnas.1319238111,
812   2014.

813 Yang, J. H., Zhang, Q., Liu, X. Y., Yue, P., Shang, J. L., Ling, H., and Li, W. J.: Spatial-temporal
814   characteristics and causes of summer precipitation anomalies in the transitional zone of
815   typical summer monsoon, China, Chinese Journal of Geophysics, 62, 4120–4128 (In
816   Chinese with English abstract), https://doi.org/10.6038/cjg2019M0639, 2019.

817 Yuan, L.: Hazards history in northwestern China, Gansu people's press, Lanzhou, China1994.

818 Zhang, F., Chen, Q. M., Su, J. J., Deng, Y., Gao, L. L., and Gou, X. H.: Tree-ring recorded of
819   the drought variability in the northwest monsoon marginal, China, Journal of Glaciology
820   and Geocryology, 39, 245–251 (In Chinese with English abstract),
821   https://doi.org/10.7522/j.issn.1000-0240.2017.0028, 2017.

822 Zhang, Q., Yang, J. H., Wang, P. L., Yu, H. P., Yue, P., Liu, X. Y., Lin, J. J., Duan, X. Y., Zhu,
823   B., and Yan, X. Y.: Progress and prospect on climate warming and humidification in
824   Northwest China, Chin. Sci. Bull., 68, 1814–1828, https://doi.org/10.1360/TB-2022-0643,
825   2023.

826 Zhang, Q. B., Cheng, G. D., Yao, T. D., Kang, X. C., and Huang, J. G.: A 2,326 year tree-ring
827   record of climate variability on the northeastern Qinghai-Tibetan Plateau, Geophys. Res.
828   Lett., 30, 1739, https://doi.org/10.1029/2003GL017425, 2003.

829 Zhang, Q. L., Liu, W. G., Liu, Y., Ning, Y. F., and Wen, Q. B.: Relationship between the stable
830   carbon and oxygen isotopic compositions of tree ring in the Mt. Helan region,

831   Northwestern China, Geochimica, 34, 51–56, https://doi.org/10.19700/j.0379-
832   1726.2005.01.006, 2005a.

833   Zhang, S., Xu, H., Lan, J. H., Goldsmith, Y., Torfstein, A., Zhang, G. L., Zhang, J., Song, Y. P.,
834   Zhou, K. E., Tan, L. C., Xu, S., Xu, X. M., and Enzel, Y.: Dust storms in northern China
835   during the last 500 years, Science China Earth Sciences, 64, 813–824,
836   https://doi.org/10.1007/s11430-020-9730-2, 2021.

837   Zhang, Y., Shao, X. M., Yin, Z. Y., Liang, E. Y., Tian, Q. H., and Xu, Y.: Characteristics of
838   extreme droughts inferred from tree-ring data in the Qilian Mountains, 1700-2005, Clim.
839   Res., 50, 141–159, https://doi.org/10.3354/cr01051, 2011.

840   Zhang, Y. X., Yu, L., and Yin, H.: Annual precipitation reconstruction over last 191 years at the
841   south edge of Badain Jaran Desert based on tree ring width data, Desert and Oasis
842   Meteorology, 9, 12–16 (In Chinese with English abstract),
843   https://doi.org/10.3969/j.issn.1002-0799.2015.01.003, 2015.

844   Zhang, Y. X., Gou, X. H., Hu, W. D., Peng, J. F., and Liu, P. X.: The drought events recorded
845   in tree ring width in Helan Mt. over past 100 years, Acta Ecologica Sinica, 25, 2121–2126
846   (In Chinese with English abstract), 2005b.

847